electronics

Communication

A Tunable Constant-Absolute-Bandwidth Bandpass Filter with Switchable Ability

Tiejun Du [1], Dujuan Wei [1,*], Pengquan Zhang [1], Boran Guan [1] and Yue Gu [2]

[1] School of Electronics & Information, Hangzhou Dianzi University, Hangzhou 310018, China; dutiejun@hdu.edu.cn (T.D.); zpq@hdu.edu.cn (P.Z.); brguan@hdu.edu.cn (B.G.)
[2] School of Automation, Zhejiang Institute of Mechanical & Electrical Engineering, Hangzhou 310053, China; guyue@zime.edu.cn
* Correspondence: weidujuan@hdu.edu.cn

Abstract: This paper presents a tunable bandpass filter (BPF) with constant absolute bandwidth (CABW) and switchable properties. The BPF is performed by using a tri-mode cross-shape resonator (CSR) loaded with varactors. The CABW and switchable ability are achieved by adjusting the resonant frequencies. Meanwhile, the two transmission zeros (TZs) produced by center-loaded stubs strengthen the skirt selectivity in the on-state and the isolation in the off-state. For demonstration, a tri-pole switchable BPF with three control voltages is implemented and verified, and the control mechanism is simple. In the on-state, it exhibits a 120 MHz, 3 dB CABW with the measured insertion loss (IL) of 2.2–2.5 dB in the tuning range of 0.816–1.188 GHz. In the off-state, the measured isolation is better than 27 dB.

Keywords: tunable; CABW; BPF; switchable; CSR

check for updates

Citation: Du, T.; Wei, D.; Zhang, P.; Guan, B.; Gu, Y. A Tunable Constant-Absolute-Bandwidth Bandpass Filter with Switchable Ability. *Electronics* **2022**, *11*, 1047. https://doi.org/10.3390/electronics11071047

Academic Editor: Federico Alimenti

Received: 28 February 2022
Accepted: 23 March 2022
Published: 27 March 2022

1. Introduction

Modern wireless communication systems require multifunctional RF front-ends in which reconfigurable filters play an essential role for easy integration. Additionally, a number of filters with tunability of center frequency (CF), bandwidth (BW) or TZs have been reported [1–7]. Furthermore, reconfigurable filters with switchable ability have attracted the attention of researchers since they are able to form switched filter banks and expand the tuning range of the filter [8–11].

By utilizing pin diodes as switches to tunable BPFs, a BPF which can switch the low- or high-tunable passband in on-state is proposed in [11], and a BPF which can switch the tunable passband in the on- or off-state is proposed in [12]. However, the use of pin diodes will make the design bulky and the control complex. To overcome this problem, intrinsically switched tunable BPFs are proposed, and the switching function is performed by using the filters' own tuning elements without additional switches. Through controlling the coupling coefficients between resonators to be zero [9,10,13], adjusting the TZs to suppress the passband [14–16], and employing transversal filter structures based on multimode resonators and modifying the resonant frequencies of odd- and even-mode to be the same [17,18], the tunable filters have the ability to switch the passband in the off-state.

On the other hand, the tunable BPFs with CABW property, which can replace a number of fixed filters and reduce the size of the communication systems, have also attracted lots of attention. By compensating the coupling coefficient with the inter-resonator varactors [19–21], choosing a proper coupling region [22,23], and maintaining the separation between resonant frequencies [18,24], tunable BPFs with CABW property have been reported.

In this letter, a tunable CABW BPF with switchable ability is proposed based on a novel CSR. The tunable CABW is accomplished by adjusting the resonant frequencies and maintaining their separations simultaneously. Moreover, the switchable ability of the passband is achieved by using its transversal filter structure. By utilizing the transmission zeros of the resonator, the skirt selectivity of the on-state and the isolation of the off-state are improved [25]. As a demonstration, a prototype of a switched tunable 120 MHz 3-dB CABW BPF with a tuning range of 0.816–1.188 GHz is developed and characterized. Experimental and simulated results are in good agreement.

2. Filter Design and Analysis

2.1. Analysis of CSR

The proposed tri-mode CSR shown in Figure 1a consists of a half-wave resonator and two shunt stubs, where Y_1, Y_2 and Y_3 are the characteristic admittances and θ_1, θ_2 and θ_3 are the electrical lengths. For tuning the resonant frequencies, three types of varactors (C_1, C_2 and C_3) are added in the resonator.

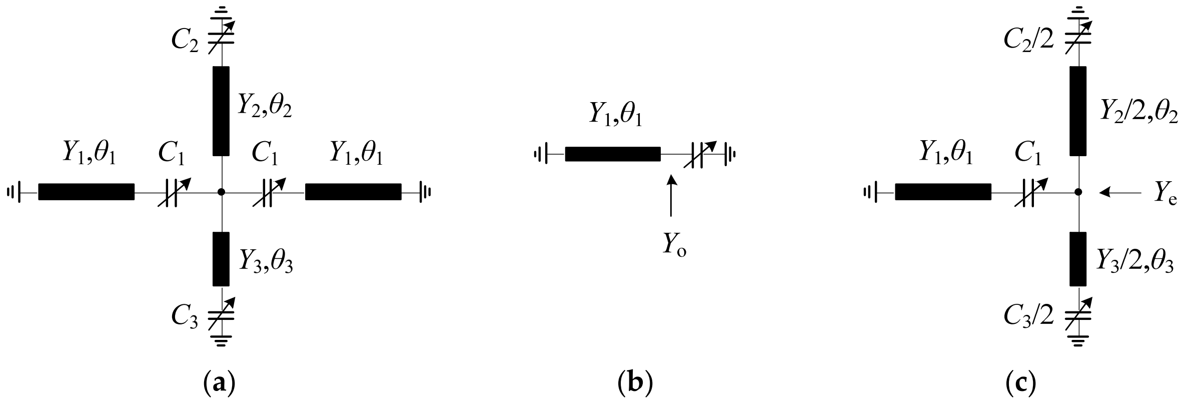

Figure 1. (**a**) Proposed CSR; (**b**) Odd-mode equivalent circuit; (**c**) Even-mode equivalent circuit.

Due to the symmetrical structure, the odd- and even-mode equivalent circuits can be expressed as shown in Figure 1b,c, respectively [26]. The input admittances of the proposed resonator can be derived as follows.

For odd-mode

$$Y_o = -jY_1\cot\theta_1 + j2\pi fC_1, \quad (1)$$

The odd-mode resonant frequency f_o can be determined according to Im (Y_o) = 0.

For even-mode

$$Y_{e1} = -jY_1\cot\theta_1 \times 2\pi fC_1/(-Y_1\cot\theta_1 + 2\pi fC_1), \quad (2)$$

$$Y_{e2} = Y_2\,(j2\pi fC_2 + jY_2\tan\theta_2)/(2Y_2 - 4\pi fC_2\tan\theta_2), \quad (3)$$

$$Y_{e3} = Y_3\,(j2\pi fC_3 + jY_3\tan\theta_3)/(2Y_3 - 4\pi fC_3\tan\theta_3), \quad (4)$$

$$Y_e = Y_{e1} + Y_{e2} + Y_{e3}, \quad (5)$$

The two even-mode resonant frequencies f_{e1} and f_{e2} can be deduced by Im (Y_e) = 0.

Based on Equations (1)–(5), Figure 2 shows the tuning range of f_o with variation of C_1, and Figure 3 plots the f_o, f_{e1} and f_{e2} dependence on C_2 and C_3 for C_1 = 1 pF. It can be observed that the odd-mode resonant frequency f_o is only controlled by C_1, and the even-mode resonant frequencies f_{e1} and f_{e2} are varied around f_o by tuning C_2 and C_3 when C_1 is fixed, that is to say, the specified frequency space between $f_{e1/e2}$ and f_o can be obtained by tuning C_2 and C_3. Note that there is a set of C_2 and C_3 makes $f_{e1} = f_o = f_{e2}$ for fixed C_1 (f_o), and this feature can be used for switching off the passband, which will be discussed in Section 2.2.

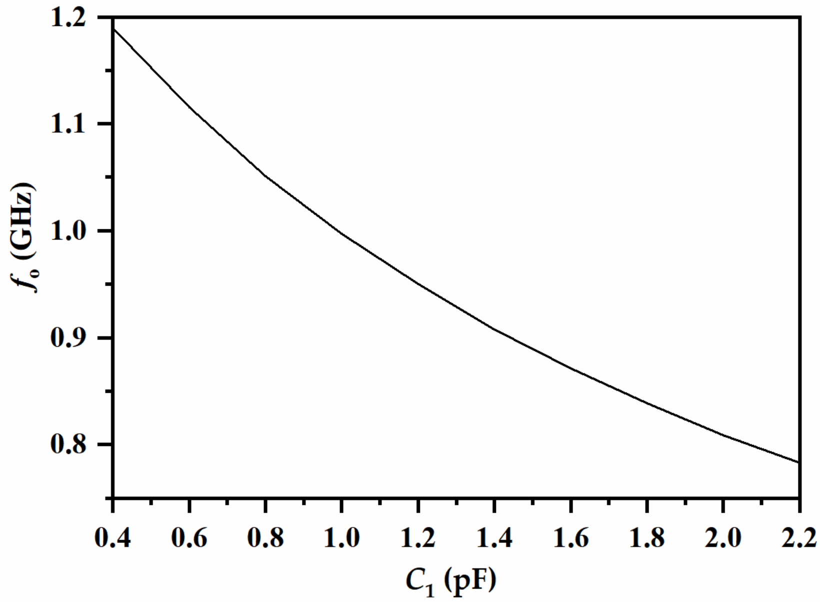

Figure 2. Odd-mode resonant frequency f_o versus C_1 (Y_1 = 1/75 S, Y_2 = Y_3 = 2/75 S, θ_1 = 65°, θ_2 = 60° and θ_3 = 35° at 1 GHz).

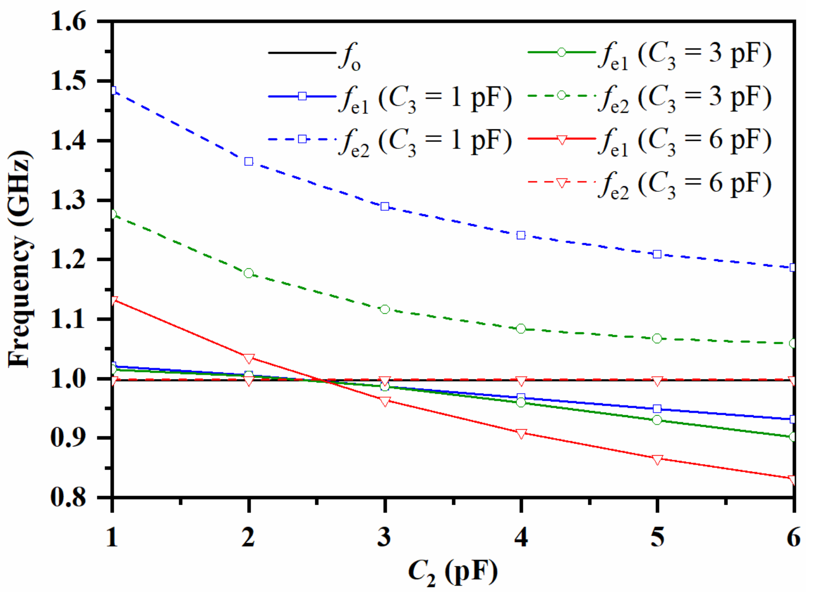

Figure 3. Resonant frequencies f_o, f_{e1} and f_{e2} versus C_2 with different C_3 (Y_1 = 1/75 S, Y_2 = Y_3 = 2/75 S, θ_1 = 65°, θ_2 = 60° and θ_3 = 35° at 1 GHz).

2.2. Coupling Matrix Analysis

Figure 4 shows the transversal topology architecture of the proposed filter, which consists of a tri-mode CSR, source, load and external quality factor Q_e. The denormalized coupling matrix can be expressed as [18]

$$[m_\Delta] = \begin{bmatrix} m_{e1e1} & 0 & 0 \\ 0 & m_{oo} & 0 \\ 0 & 0 & m_{e2e2} \end{bmatrix}, \tag{6}$$

where $m_{e1e1/oo/e2e2} = f_d/f_{e1/o/e2} - f_{e1/o/e2}/f_d$, f_d is the frequency-mapping element.

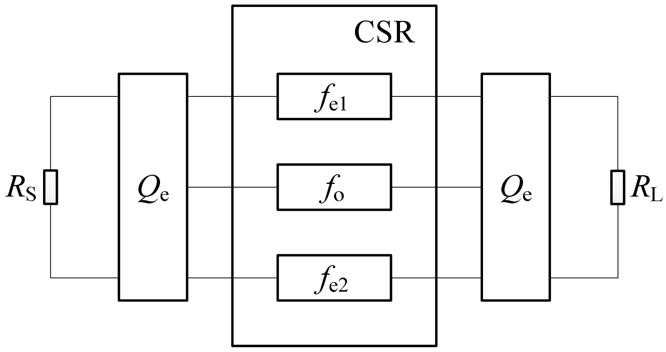

Figure 4. Topology architecture of the proposed filter.

The external quality factor can be expressed as [27]

$$Q_e = (Q_{exe1} + Q_{exe2} + Q_{exo})/3, \quad (7)$$

$$Q_{exe1/exe2/exo} = f_{e1/e2/o}/\Delta f_{e1/e2/o\pm 90^\circ}, \quad (8)$$

where $Q_{exe1/exe2/exo}$ and $\Delta f_{e1/e2/o\pm 90^\circ}$ are the external quality factor and BW of the three resonant modes, respectively.

By separately tuning the parameters of the coupling matrix and Q_e, the theoretical response curves with f_d = 1 GHz are given in Figures 5–7 [18,28]. Figure 5 displays the theoretical response curves varying m_{e1e1}, m_{oo} and m_{e2e2} considering a fixed Q_e = 28. As can be seen, center frequency tuning behavior with CABW property can be obtained by purposely changing the variable elements in the coupling matrix. As shown in Figure 6, the specified 3 dB BW can be achieved by adjusting the frequency space between $f_{e1/e2}$ and f_o, and $BW_{3dB} \approx f_{e2} - f_{e1}$ when $f_{e2} > f_o > f_{e1}$. In particular, when $m_{e1e1} = m_{e2e2} = m_{oo} = 0$ (i.e., $f_{e1} = f_o = f_{e2}$), the passband is switched off. Figure 7 illustrates the calculated frequency responses when Q_e is tuned from 40 to 10 but the elements of the coupling matrix are fixed as $m_{e1e1} = -m_{e2e2} = 0.15$ and $m_{oo} = 0$. The return loss (RL) of the passband increases when Q_e decreases, and the 3 dB BW of the passband is almost independent of Q_e when Q_e varies from 40 to 20, but as Q_e continues to decrease, the 3 dB BW becomes narrower and cannot be estimated as $f_{e2} - f_{e1}$. As a conclusion, the specified BW and off-state of the passband can be controlled by f_{e1}, f_o and f_{e2}, and a range of Q_e provide controllable BW with a RL of the passband better than a certain value.

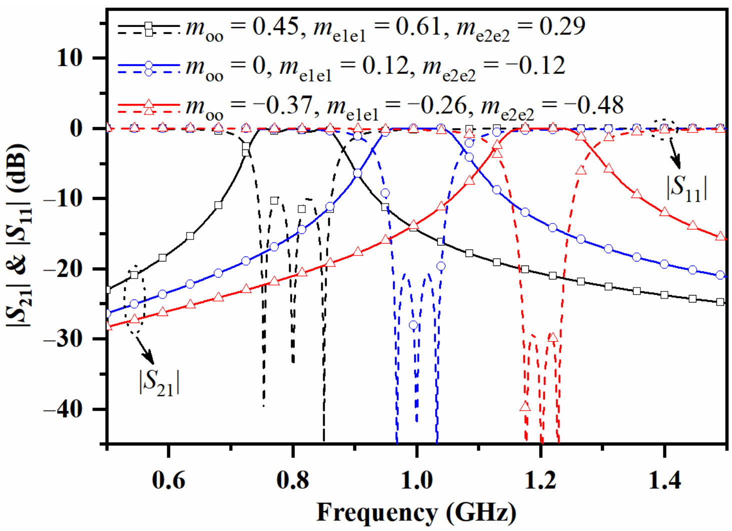

Figure 5. Theoretical curves for varying m_{e1e1}, m_{oo} and m_{e2e2} considering a fixed Q_e = 28.

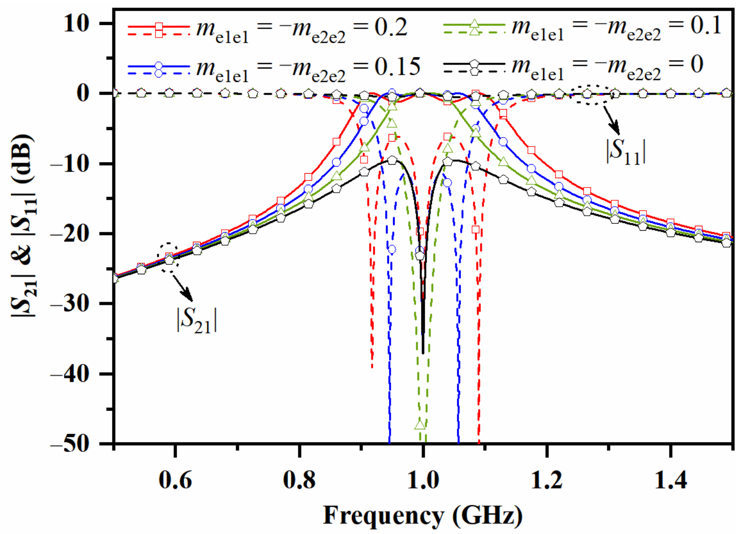

Figure 6. Theoretical curves for varying m_{e1e1} and m_{e2e2} with fixed m_{oo} = 0 and Q_e = 28.

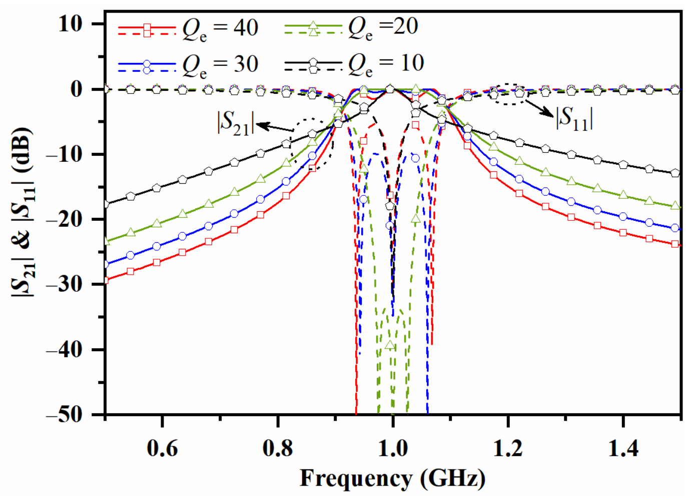

Figure 7. Theoretical curves for varying Q_e considering $m_{e1e1} = -m_{e2e2}$ = 0.15 and m_{oo} = 0.

2.3. Analysis of TZs

The two shunt stubs taped with C_2 and C_3 can produce two TZs, respectively. The input admittances of the two stubs are as below.

$$Y_d = Y_2\,(j2\pi f C_2 + jY_2\tan\theta_2)/(Y_2 - 2\pi f C_2\tan\theta_2), \tag{9}$$

$$Y_u = Y_3\,(j2\pi f C_3 + jY_3\tan\theta_3)/(Y_3 - 2\pi f C_3\tan\theta_3), \tag{10}$$

The frequencies of the two TZs f_{z1} and f_{z2} can be deduced by $Y_2 - 2\pi f C_2\tan\theta_2 = 0$, and $Y_3 - 2\pi f C_3\tan\theta_3 = 0$, respectively [29]. As can be seen, f_{z1} and f_{z2} are controlled by C_2 and C_3, respectively.

In Figure 8, the weak coupling transmission responses are investigated when $Y_1 = Y_2/2 = Y_3/2 = 1/75$ S, $\theta_1 = 65°$, $\theta_2 = 60°$ and $\theta_3 = 35°$ at 1 GHz. Seen from Figure 8, the condition of $f_{z1} < f_{e1} < f_o < f_{e2} < f_{z2}$ can be realized, and the two TZs can be utilized to improve the out-of-band rejection. By increasing C_2 and decreasing C_3, the BW ($f_{e2} - f_{e1}$) becomes narrower and the two TZs follow the variations of f_{e1} and f_{e2}. When $f_{e1} = f_o = f_{e2}$ is realized by tuning C_2 and C_3, the two TZs are also tuned to the same frequency as f_o and can be used to enhance the isolation of the off-state.

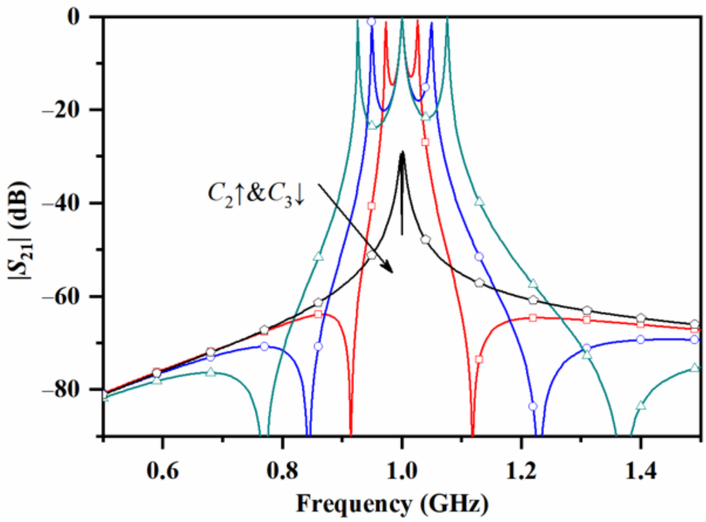

Figure 8. Transmission responses using weak coupling.

2.4. Schematic Diagram of the Filter and the External Quality Factor

Figure 9 presents the schematic diagram of the reconfigurable BPF based on the CSR proposed in this paper. The BPF consists of a CSR and a pair of feedlines. The three resonant modes of the CSR are utilized to form the three poles of the filter, and the two transmission zeros of the CSR are used to improve the skirt selectivity of the filter in on-state and the isolation in off-state. The variable capacitors are realized by varactors, and several lumped components are employed for DC blocks (C_b = 30 pF) and DC bias (R_b = 10 kΩ). The voltages V_1, V_2 and V_3 are utilized to tune the capacitances of the varactors. Due to the influence of C_b, the relationship between C_i in Figure 1 and C_{vi} (i = 1, 2, 3) in Figure 9 are $C_1 = C_{v1}$, $C_2 = C_bC_{v2}/(C_b + C_{v2})$ and $C_3 = C_bC_{v3}/(C_b + C_{v3})$.

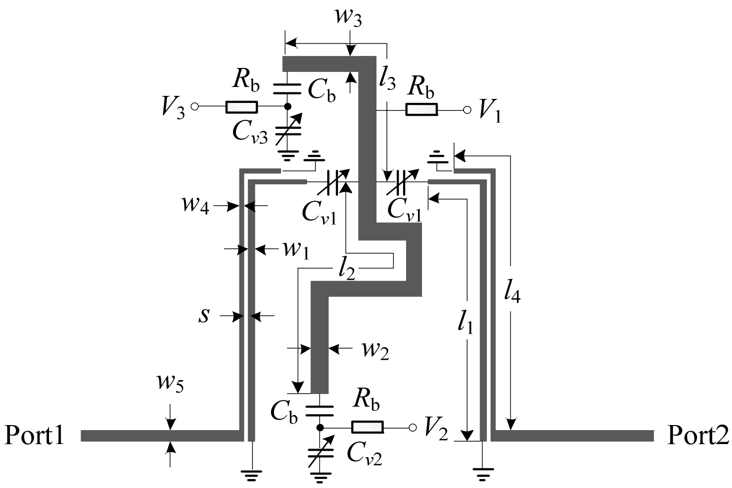

Figure 9. Schematic diagram of the proposed filter.

Based on the discussion in Section 2.2, the desired Q_e for realizing a BPF with 120 MHz 3 dB BW in the frequency range of 0.8–1.2 GHz is illustrated in Figure 10, where Q_{emax} is the maximum external quality factor, with which the RL of the passband is better than 10 dB, and Q_{emin} is the minimum external quality factor, with which the 120 MHz 3 dB BW of the passband can be estimated by $f_{e2} - f_{e1}$. Therefore, Q_e between Q_{emin} and Q_{emax} can be utilized to realize a passband with following characteristics: dB$|S_{11}| < -10$ dB and $BW_{3dB} \approx f_{e2} - f_{e1}$ = 120 MHz.

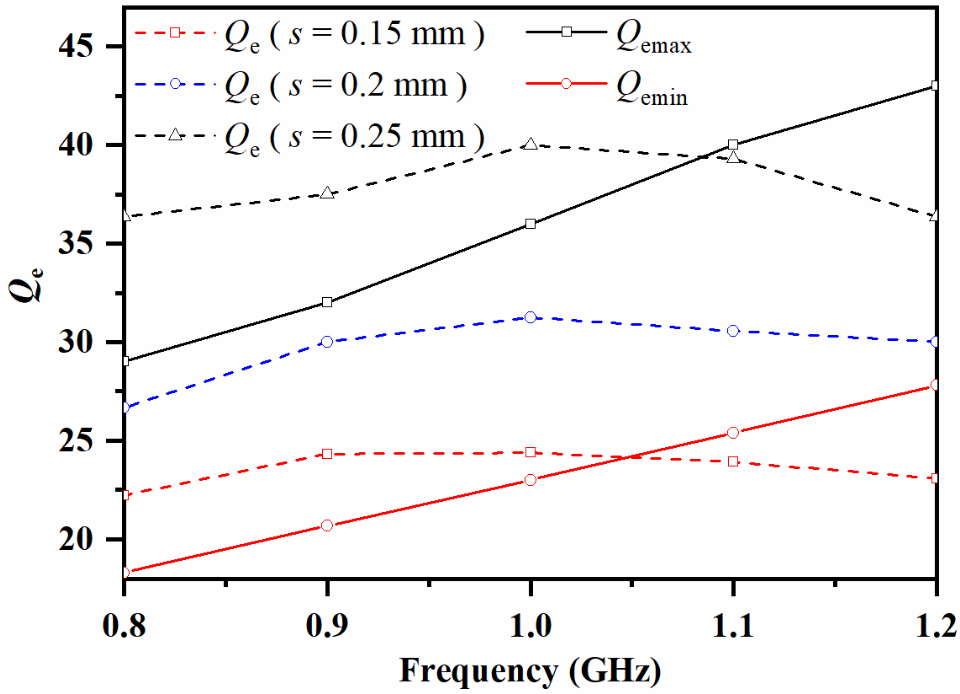

Figure 10. Desired and extracted Q_e.

Q_e curves with different distance s in the frequency range of 0.8–1.2 GHz are extracted by Equations (7) and (8) and shown in Figure 10. When frequency is changed from 0.8 to 1.2 GHz, the Q_e curve changes from increasing to decreasing, and when s is adjusted from 0.15 to 0.25 mm, the Q_e curve moves from a small value to large. Apparently, Q_e (s = 0.2 mm) is in the range between Q_{emin} and Q_{emax} in the frequency range of 0.8–1.2 GHz and can be used to design the tunable BPF with 120 MHz 3 dB BW.

3. Experimental Verification

The reconfigurable BPF is fabricated on a 0.508 mm RO4003C substrate with a relative dielectric constant of 3.55 and a loss tangent of 0.0027. The EM simulator SONNET is employed for the physical dimension optimization, and the final physical parameters of the filter are determined as in Table 1. C_b = 30 pF and R_b = 10 kΩ are used as DC block and DC bias, respectively. The varactors Ma46H201 from M/A COM are employed as C_{v1}s, the varactors Ma46H202 from M/A COM are employed as C_{v2} and C_{v3}, and the voltages V_1, V_2 and V_3 are utilized to control the capacitances of C_{v1}s, C_{v2} and C_{v3}, respectively. The photography of the fabricated reconfigurable BPF is presented in Figure 11. The size of the filter is approximately 0.09 λg × 0.18 λg, where λg is the guided wavelength on the substrate at 0.816 GHz.

Table 1. Physical parameters of the proposed filter.

Parameter	Value (mm)	Parameter	Value (mm)
l_1	31.6	w_1	0.5
l_2	33.6	w_2	1.5
l_3	19.2	w_3	1.5
l_4	28.8	w_4	0.5
s	0.18	w_5	1.1

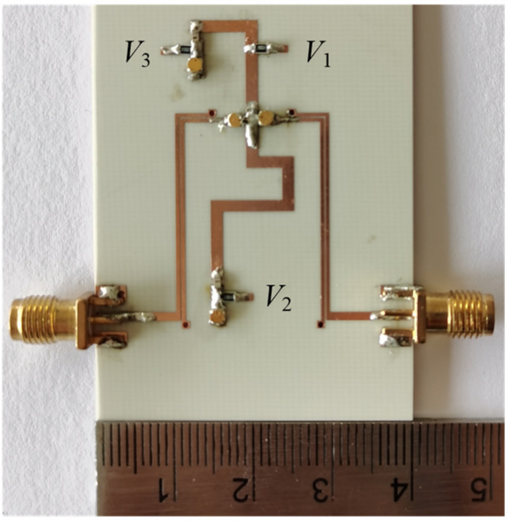

Figure 11. Photograph of the fabricated filter.

The measurement is performed with a Rohde & Schwarz ZVA24 analyzer. The measurement results are compared with the simulation results as shown in Figures 12 and 13. Figure 12 shows the results of the filter as a CABW tunable filter with a 3 dB BW of 120 MHz. The center frequency can vary from 0.816 to 1.188 GHz and the measured 3 dB BW of the filter is 120 ± 2 MHz, the measured IL is 2.2–2.5 dB, and the measured RL is better than 10 dB over the tuning range. The IL is dominated by the parasitic resistances of the varactors [3]. Two TZs on either side of the passband improve the skirt selectivity. Figure 13 shows the results of the filter in the off-state. As can be seen, the measured isolation is better than 27 dB. A comparison with other tunable CABW BPFs presented in previous studies is provided in Table 2. The tunable CABW BPFs proposed in [20,23] have no switchable ability. The switchable ability of the filter proposed in [12] is realized by using PIN diodes, therefore, extra bias voltages are needed in the design and the IL is poor. The number of the control voltages is the same as the order of the proposed filter in [17], which makes its control simplistic, however, the isolation of its off-state is poor. The two-pole tunable CABW filter in [18] presents a minimum 20 dB isolation of its off-state, but the number of the control voltages is four. In this study, the tunable CABW filter presents low IL in the on-state and high isolation in the off-state, and the tri-pole BPF with switchable ability using only three bias voltages, which simplifies the control complexity.

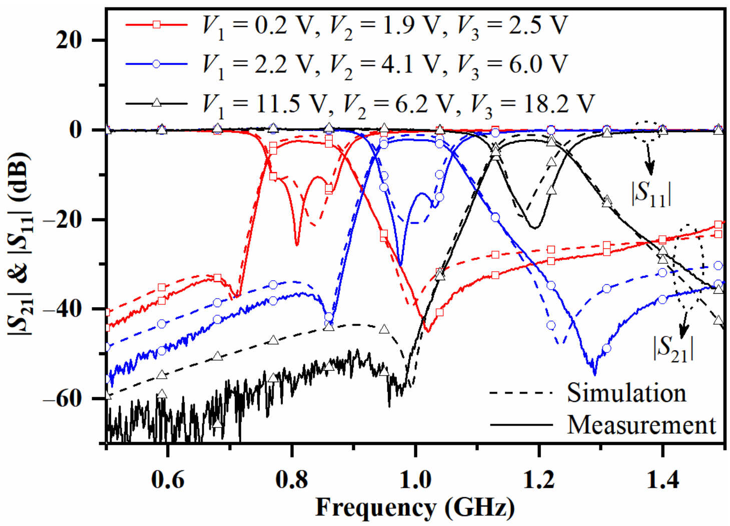

Figure 12. Simulated and measured S parameters for the proposed filter in on-state.

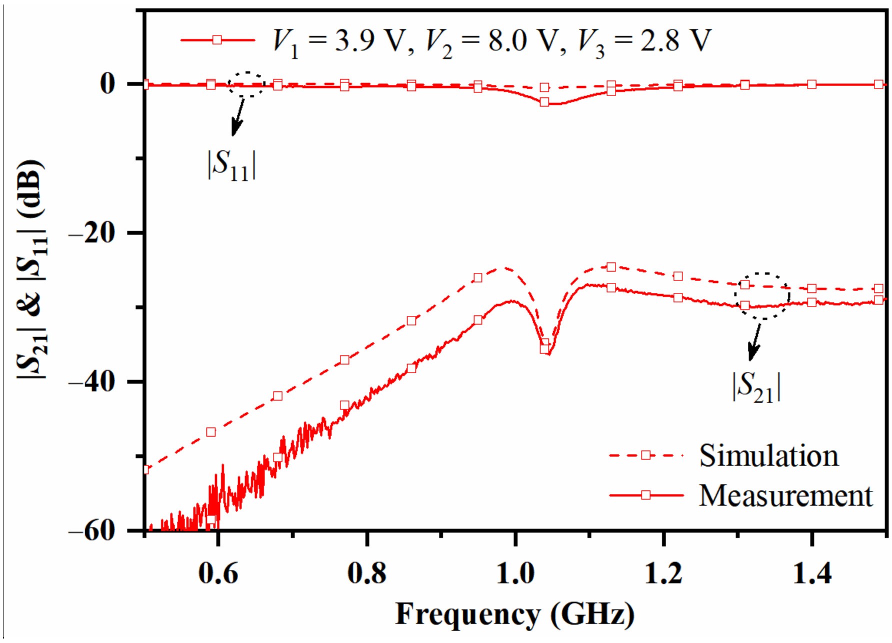

Figure 13. Simulated and measured S parameters for the proposed filter in off-state.

Table 2. Comparisons with previously reported tunable CABW filters.

Ref No.	Filter Order	Number of Control Voltages	IL in Passband (dB)	Off-State	Isolation in Off-State (dB)	Size (λ_g^2)
[20]	2	3	1.2–2.3	No	-	0.0042
[23]	2	1	1.34–2.92	No	-	0.0224
[12]	2	3	2.52–4.08	Yes	>43	0.0183
[17]	2	2	1–3	Yes	>10	0.0121
[18]	2	4	≤3.8	Yes	>20	0.0211
This work	3	3	2.2–2.5	Yes	>27	0.0162

4. Conclusions

This letter proposed a tri-pole reconfigurable CABW BPF with switchable ability. The CSR loaded with varactors is employed to make the tunable element, and the center-loaded stubs in the CSR are utilized to generate the two TZs and improve the selectivity of the filter. Coupling matrix analysis of the transversal filter structure shows that center frequency tuning CABW and switchable ability can be achieved through adjusting the resonant frequencies. The weak coupling transmission-line responses demonstrate that the TZs can be used to improve the isolation of the off-state. Center frequency tuning, CABW maintenance, and switchable ability of the tri-pole filter are realized by using only three control variables, which simplifies the control complexity. The proposed filter has the potential to be applied in switched filter banks to reduce control complexity.

Author Contributions: Conceptualization, T.D. and B.G.; Experiment, T.D. and Y.G.; writing—original draft preparation, T.D.; writing—review and editing, D.W. and P.Z.; supervision, D.W. All authors have read and agreed to the published version of the manuscript.

Funding: This work was supported by the National Natural Science Foundation of China under grant number 61801153, Zhejiang Provincial Natural Science Foundation of China under grant number LQ22F010014 and Fundamental Research Funds for the Provincial Universities of Zhejiang under grant number GK219909299001-024.

Conflicts of Interest: The authors declare no conflict of interest.

References

1. Brito-Brito, Z.; Llamas-Garro, I.; Pradell, L. Selectivity-tuned bandpass filter. *Electron Lett.* **2009**, *45*, 984–985. [CrossRef]
2. Miller, A.; Hong, J. Wideband bandpass filter with reconfigurable bandwidth. *IEEE Microw. Wireless Compon. Lett.* **2010**, *20*, 28–30. [CrossRef]
3. Chen, J.X.; Ma, Y.; Cai, J.; Zhou, L.H.; Bao, Z.H.; Che, W. Novel frequency-agile bandpass filter with wide tuning range and spurious suppression. *IEEE Trans. Ind. Electron.* **2015**, *62*, 6428–6435. [CrossRef]
4. Qin, W.; Cai, J.; Li, Y.; Chen, J. Wideband tunable bandpass filter using optimized varactor-loaded SIRs. *IEEE Microw. Wireless Compon. Lett.* **2017**, *7*, 812–814. [CrossRef]
5. Cheng, T.; Tam, K. A wideband bandpass filter with reconfigurable bandwidth based on cross-shaped resonator. *IEEE Microw. Wireless Compon. Lett.* **2017**, *27*, 909–911. [CrossRef]
6. Cheng, F.; Li, X.T.; Lu, P.; Huang, K. A microstrip bandpass filter with 2 independently tunable transmission zeros. *Microw. Opt. Technol. Lett.* **2020**, *62*, 1951–1956. [CrossRef]
7. Fan, M.; Song, K.; Fan, Y. Reconfigurable bandpass filter with wide-range bandwidth and frequency control. *IEEE Trans. Circuits Syst. II Exp. Briefs* **2021**, *68*, 1758–1762. [CrossRef]
8. Sun, J.S.; Kaneda, N.; Baeyens, Y.; Itoh, T.; Chen, Y.K. Multilayer planar tunable filter with very wide tuning bandwidth. *IEEE Trans. Microw. Theory Tech.* **2011**, *59*, 2864–2871. [CrossRef]
9. Guyette, A.C. Intrinsically switched varactor-tuned filters and filter banks. *IEEE Trans. Microw. Theory Tech.* **2012**, *60*, 1044–1056. [CrossRef]
10. Cho, Y.H.; Rebeiz, G.M. Tunable 4-pole noncontiguous 0.7–2.1-GHz bandpass filters based on dual zero-value couplings. *IEEE Trans. Microw. Theory Tech.* **2015**, *63*, 1579–1586. [CrossRef]
11. Lin, F.; Rais-Zadeh, M. Continuously tunable 0.55–1.9-GHz bandpass filter with a constant bandwidth using switchable varactor-tuned resonators. *IEEE Trans. Microw. Theory Tech.* **2017**, *65*, 792–803. [CrossRef]
12. Zhang, Y.; Cai, J.; Chen, J. Design of novel reconfigurable filter with simultaneously tunable and switchable passband. *IEEE Access* **2019**, *7*, 59708–59715. [CrossRef]
13. Yang, T.; Rebeiz, G.M. Tunable 1.25-2.1-GHz 4-pole bandpass filter with intrinsic transmission zero tuning. *IEEE Trans. Microw. Theory Tech.* **2015**, *63*, 1569–1578. [CrossRef]
14. Psychogiou, D.; Gómez-García, R.; Peroulis, D. Tune-all RF planar duplexers with intrinsically switched channels. *IEEE Microw. Wireless Compon. Lett.* **2017**, *27*, 350–352. [CrossRef]
15. Psychogiou, D.; Gómez-García, R.; Peroulis, D. Fully-reconfigurable bandpass/bandstop filters and their coupling-matrix representation. *IEEE Microw. Wireless Compon. Lett.* **2016**, *26*, 22–24. [CrossRef]
16. Gómez-García, R.; Muñoz-Ferreras, J.; Psychogiou, D. Dual-behavior resonator-based fully reconfigurable input reflectionless bandpass filters. *IEEE Microw. Wireless Compon. Lett.* **2019**, *29*, 35–37. [CrossRef]
17. Serrano, A.L.C.; Correra, F.S.; Vuong, T.P.; Ferrari, P. Synthesis methodology applied to a tunable patch filter with independent frequency and bandwidth control. *IEEE Trans. Microw. Theory Tech.* **2012**, *60*, 484–493. [CrossRef]
18. Lu, D.; Tang, X.; Barker, N.S.; Yan, T. Synthesis-applied highly selective tunable dual-mode BPF with element-variable coupling matrix. *IEEE Trans. Microw. Theory Tech.* **2018**, *66*, 1804–1816. [CrossRef]
19. Chi, P.L.; Yang, T.; Tsai, T.Y. A fully tunable two-pole bandpass filter. *IEEE Microw. Wireless Compon. Lett.* **2015**, *25*, 292–294. [CrossRef]
20. Kumar, N.; Singh, Y.K. Compact constant bandwidth tunable wideband BPF with second harmonic suppression. *IEEE Microw. Wireless Compon. Lett.* **2016**, *26*, 870–872. [CrossRef]
21. Chen, C.F.; Wang, G.Y.; Li, J.J. Microstrip switchable and fully tunable bandpass filter with continuous frequency tuning range. *IEEE Microw. Wireless Compon. Lett.* **2018**, *28*, 500–502. [CrossRef]
22. Zhang, X.Y.; Xue, Q.; Chan, C.H.; Hu, B.J. Low-loss frequency-agile bandpass filters with controllable bandwidth and suppressed second harmonic. *IEEE Trans. Microw. Theory Tech.* **2010**, *58*, 1557–1564. [CrossRef]
23. Cai, J.; Chen, J.X.; Zhang, X.F.; Yang, Y.J.; Bao, Z.H. Electrically varactor-tuned bandpass filter with constant bandwidth and self-adaptive transmission zeros. *IET Microw. Antennas Propag.* **2017**, *11*, 1542–1548. [CrossRef]
24. Jung, M.; Min, B.W. A widely tunable compact bandpass filter based on a switched varactor tuned resonator. *IEEE Access* **2019**, *7*, 95178–95185. [CrossRef]
25. Hookari, M.; Roshani, S.; Roshani, S. Design of a low pass filter using rhombus-shaped resonators with an analytical LC equivalent circuit. *Turk. J. Electr. Eng. Comp. Sci.* **2020**, *28*, 865–874. [CrossRef]
26. Tang, W.; Hong, J.S. Varactor-tuned dual-mode bandpass filters. *IEEE Trans. Microw. Theory Tech.* **2010**, *58*, 2213–2219. [CrossRef]
27. Lu, D.; Tang, X.; Barker, N.S.; Feng, Y. Single-band and switchable dual-/single-band tunable BPFs with predefined tuning range, bandwidth, and selectivity. *IEEE Trans. Microw. Theory Tech.* **2018**, *66*, 1215–1227. [CrossRef]
28. Cameron, R.J. Advanced coupling matrix synthesis techniques for microwave filters. *IEEE Trans. Microw. Theory Tech.* **2003**, *51*, 1–10. [CrossRef]
29. Ma, Y.L.; Che, W.; Chen, J.X.; Feng, W. High selectivity balanced bandpass filter with tunable bandwidth using stub-loaded resonator. *Prog. Electromagn. Res. Lett.* **2015**, *55*, 89–95. [CrossRef]